Polymer Chemistry

Accepted Manuscript

ROYAL SOCIETY OF CHEMISTRY

www.rsc.org/polymers

Enhanced Performance for Organic Bulk Heterojunction Solar Cells by Cooperative Assembly of Ter(ethylene Oxide) Pendant

Lie Chen[1], Shaojie Tian[1], Yiwang Chen[*1,2]

[1]Institute of Polymers/Department of Chemistry, Nanchang University, 999 Xuefu Avenue, Nanchang 330031, China; [2]Jiangxi Provincial Key Laboratory of New Energy Chemistry, Nanchang University, 999 Xuefu Avenue, Nanchang 330031, China

ABSTRACT

Two ter(ethylene oxide) (TEO) functionalized copolymer donor and fullerene acceptor, namely poly{4,8-bis(5-(2-ethylhexyl)thiophen-2-yl)benzo[1,2-b: 4,5-b']dithiophene-alt-4,6-thieno[3,4-b]thiophene-2-carboxylic acid 2-[2-(2-methoxy-ethoxy)-ethoxy]-ethyl ester} (PBDTT-TT-TEO) and [6,6]-phenyl C_{61} butyric acid 2-[2-(2-methoxy- ethoxy)- ethoxy]-ethyl ester (PCB-TEO), respectively, are explored to manipulate the self-assembly nanoscale morphology and enhance stability of photoactive layer in polymer solar cells. Compared with the copolymer PBDTT-TT, TEO side chains induces PBDTT-TT-TEO with more ordered molecular packing, leading to the PCE of device improved from 3.6% for PBDTT-TT:PCBM to 4.1% for PBDTT-TT-TEO:PCBM. Directly blending PBDTT-TT-TEO with PCB-TEO as the active layer does not afford high performance of device due to the discontinuous morphology of blend film caused by the poor solubility of the PCB-TEO. However, precisely controlling the loadings of PCB-TEO in PBDTT-TT-TEO:PCBM blend greatly promotes the PCE of device, because the TEO modified fullerene can serve as an effective compatibilizer to well manipulate the miscibility between the polymer donor and acceptor and achieve favorable heterojunction morphology by cooperative assembly effect. The device with 5% loading of PCB-TEO achieves the highest PCE of 4.8%, with a J_{sc} of 12.18 mA/cm^2, a V_{oc} of 0.722 V and a FF of 55.0%, approximately 33% improvement in PCE over PBDTT-TT:PCBM device. In addition, PCB-TEO compatibilizer located at the interface of donor and acceptor strengths the

* Corresponding author. Tel.: +86 791 83969562; fax: +86 791 83969561. *E-mail address*: ywchen@ncu.edu.cn (Y. Chen).

interaction of PBDTT-TT-TEO with PCBM, consequently improving the morphological and device stability.

Keywords: Cooperative assembly; Compatibilizer; Morphology; Polymer solar cells

Introduction

Polymer solar cells (PSCs) have attracted much attention due to their potential applications in making large-area, lightweight and flexible photovoltaic devices through roll-to-roll printing.[1-5] The bulk hetero-junction (BHJ) polymer solar cells, whose photoactive layer is composed of an interpenetrating network of electron donor materials and electron acceptor materials, have been one of the most successful device structures to date.[6-12] Recently, the power conversion efficiency (PCE) over 7% can be effortlessly reached in the research field of PSCs.[13-15] Nanomorphology of the active layer is one of the most important factors that influence the efficiency of the polymer solar cells. In optimized BHJ polymer solar cells, phase separation of donor (D) and acceptor (A) materials should be on the same length-scale as the exciton diffusion length to facilitate efficient exciton harvesting and separation. Therefore, the local conjugated polymer ordering, acceptor agglomeration and the phase separation between the donor and acceptor are directly correlated to the performance of devices.

The addition of chemical additives,[16-18] thermal annealing treatments, and solvent annealing[19] are among the frequently-used post-treatments for controlling the morphology in polymer/fullerene BHJ solar cells. Beyond these post-treatments, chemically structural modification on active layers is regarded as an effective strategy for developing the desirable microphase separation morphology of the active layers. Previous studies find that incorporation of alkoxy side chains into active layers, especially ter(ethylene oxide) (TEO) chains, show several advantages over alkyl groups.[20-25] Firstly, alkoxy chains will not cause a disadvantageous steric twist of the conjugated polymer out of planarity, which is beneficial to transport charge and can lead to higher carrier mobility.[25, 26] Secondly, TEO derivatives can generally lead to good crystallinity[27], which is quite important to optimize the morphology of the active layers. Besides, polymers loaded with alkoxy chains have commendable solubility in common solvents[25, 26], such as chloroform, chlorobenzene and orthodichloro-benzene, which makes it convenient and potential to use them in organic solar cells.

The lifetime of solar devices also importantly affects their commercialization. In fact, most PSCs devices show poor stability and often undergo macrophase segregation of the blend components, especially after prolonged exposure to heat[28]. However, the morphology of the D-A blends is normally very sensitive to the fabrication procedures and the heating process, and cannot be maintained over long operation times. Several strategies for improving the morphological stability of polymer solar cells have been developed. Exploring thermo-cleavable polymers is one of useful solutions to improve the stability of PSCs,[29] but it involves complicated synthetic routes and costs massively, which limits its applications in large-area solar cells. Using crosslinkable materials to cross-link the active layer is another approach for device stability improvement.[30-32] However, the existence of these cross-linkable moieties reduces the probability that molecules come into close contact with each other, thereby lowering the mobility of electrons in the material.[33]

To simultaneously achieve the favorable and stable morphology of active layer, herein, TEO functionalized copolymer donor PBDTT-TT-TEO and fullerene acceptor PCB-TEO are explored (**Scheme 1 and Scheme 2**). The copolymer poly{4,8-bis(5-(2-ethylhexyl)thiophen-2-yl)benzo[1,2-b:4,5-b']dithiophene-alt-4,6-thieno[3,4-b] thiophen-2-yl-2-ethylhexan-1-one} (PBDTT-TT) without TEO side chains is also synthesized for the comparison. We hope that the cooperative assembly of the donor and acceptor via the interchain interaction between the TEO side chains can construct a microphase separation nanostructure with promoted stability for high efficient PSCs. Unexpectedly, directly blending PBDTT-TT-TEO with PCB-TEO as the active layer, only affords 2.8% PCE of the device, due to the discontinuous morphology of blend film caused by the poor solubility of the PCB-TEO. However, a appropriate amount of the PCB-TEO as a compatibilizer incorporated into the PBDTT-TT-TEO:PCBM blend can dramatically improve the device performance and stability, because PCB-TEO, chemically similar to the segments in PBDTT-TT-TEO and PCBM, can locate at the interface of donor and acceptor to well manipulate the miscibility

between the polymer and fullerene and achieve a favorable and stable BHJ morphology by cooperative assembly effect. The device with 5% loading of PCB-TEO achieves the highest PCE of 4.8%, approximately 33% improvement in PCE over PBDTT-TT:PCBM device.

Results and Discussion

The synthetic routes of the copolymers PBDTT-TT-TEO and PBDTT-TT are outlined in **Scheme 1**. 4,6-dibromo-thieno[3,4-b] thiophene-2-carboxylic acid was reacted with TEO via esterification reaction to yield monomer 4,6-dibromo-thieno[3,4-b] thiophene-2-carboxylic acid 2-[2-(2-methoxy-ethoxy)- ethoxy]-ethyl ester (TT-TEO). In the presence of a catalytic amount of $Pd(PPh_3)_4$, TT-TEO was reacted with 2,6-bis(trimethyltin)-4,8-bis (5-(2-ethylhexyl)thiophen-2-yl) benzo[1,2-b:4,5-b′] dithiophene (BDTT) to afford the polymer PBDTT-TT-TEO through Stille coupling. PBDTT-TT was also synthesized following the same method as PBDTT-TT-TEO. The structures of the monomer TT-TEO and copolymers have been confirmed by ^{1}H NMR, as shown in **Figure S1** and **Figure S2**. Compared with the PBDTT-TT, copolymer PBDTT-TT-TEO shows the characteristic resonance peaks of TEO from 3.2 to 4.0, indicating the successfully synthesis of the copolymer. The molecular weights were estimated by gel permeation chromatography (GPC) using tetrahydrofuran as the eluent, and the related data is summarized in **Table 1**. PCB-TEO was synthesized from PCBM by two steps according to the literature,[24] and the synthetic procedures are provided in **Scheme 2**. The structure of PCB-TEO was also verified by ^{1}H NMR, and the data is showed in **Figure S3.** Unfortunately, PCB-TEO shows relatively poor solubility in common organic solvents, especially in chlorobenzene and orthodichlorobenzene.

Thermal properties of the copolymers were determined by thermogravimetric analysis (TGA) under nitrogen atmosphere at a heating rate of 10 ^{o}C min^{-1} (**Figure S4**). The temperature of 5% weight loss is chosen as onset point of decomposition (Td). Similar

to the polymer PBDTT-TT, PBDTT-TT-TEO almost shows little weight loss when heated up to 366 ºC, suggesting that introduction of TEO chains into the PBDTT-TT does not influence the thermal stability of the polymer. Evidently, it is sufficient for the applications in BHJ solar cells and other optoelectronic devices.

Figure 1 shows the UV-vis absorption of PBDTT-TT and PBDTT-TT-TEO films. The absorption spectrum of PBDTT-TT film shows maximum absorption at 696 nm, while PBDTT-TT-TEO film shows the highest peak at 701 nm. The slightly red shifted band of PBDTT-TT-TEO indicates that PBDTT-TT-TEO possesses bigger efficient conjugation length than PBDTT-TT. This is because TEO side chains can reduce the detrimental steric twist of the polymer out of planarity, which will be beneficial for the π–π stacking.[34]

Electrochemical cyclic voltammetry (CV) has been widely employed to investigate the electrochemical behavior of the polymers and estimate their highest occupied molecular orbital (HOMO) and lowest unoccupied molecular orbital (LUMO) energy levels. The HOMO and LUMO energy levels of the polymers were calculated from the onset oxidation potential and the onset reduction potential according to the equations in the reported literature.[35] **Figure S5** shows the cyclic voltammogram curves of the two copolymers. PBDTT-TT and PBDTT-TT-TEO possess almost identical electrochemical redox characteristics. For PBDTT-TT, the onset potential for oxidation is located around 0.27V versus $Ag/AgNO_3$, which corresponds to a highest occupied molecular orbital of -5.09 eV. The LUMO energy level of PBDTT-TT is calculated to be -3.22 eV based on the onset potential for reduction at around -1.60 V. Using similar methods, the HOMO and LUMO energy levels for PBDTT-TT-TEO are -5.07 and -3.23 eV, respectively. From the results, we can draw a conclusion that PBDTT-TT-TEO has a relatively narrower band gap than PBDTT-TT, which is in line with the result of the UV-vis spectra.

Because polymer chain packing can affect exciton dissociation, recombination and

charge transport,[36] the crystalline structures of donor/acceptor films blended with different amounts of addictive were observed by XRD measurement. **Figure S6** shows the XRD patterns of PBDTT-TT and PBDTT-TT-TEO. Both polymers show crystalline diffraction peaks at low angle (~5.0^{o}), attributed to a lamellar structure. The crystalline diffraction peak of PBDTT-TT-TEO is slightly sharper than that of PBDTT-TT, meaning that PBDTT-TT-TEO has more ordered molecular packing structure, which is consistent with the UV observation.

To determine the photovoltaic property of the TEO functionalized copolymer, the BHJ devices based on PBDTT-TT-TEO:PCBM are fabricated, and the device based on PBDTT-TT blended with PCBM is also provided for comparison. The configuration of device is glass/ITO/PEDOT:PSS/copolymer:PCBM/LiF/Al. **Figure 2** shows the I-V curves for solar cells under simulated AM 1.5 G radiation (100 mW/cm^2); optimized photovoltaic properties are summarized in **Table 2**. All of devices based on PBDTT-TT-TEO:PCBM with different weight ratios receive better performance than those based on PBDTT-TT:PCBM. The best PCE of 4.1% is obtained from the device based on PBDTT-TT-TEO:PCBM at a weight ratio of 1:2, together with a short-circuit current (J_{sc}) of 11.63mA/cm^2, an open-circuit voltage (V_{oc}) of 0.727 V and a fill factor (FF) of 48.1%, while the device based on PBDTT-TT:PCBM (1:2, w/w) obtains a inferior PCE of 3.6%, with J_{sc} of 11.09 mA/cm^2, a V_{oc} of 0.726 V and a FF of 44.5%. The improved PCE is related to the enhanced J_{sc} and FF, which should arise from the more ordered molecular packing structure of PBDTT-TT-TEO， resulting in more efficient carriers transport in the active layer.

To further improve the PCE, the device based on PBDTT-TT-TEO blended with PCB-TEO containing the same functional group was fabricated. By this way, the cooperative assembly of TEO chains in both donor and acceptor would develop the ordered microphase-separation nanomorphology for PCE enhancement. Unexpectedly, the devices based on PBDTT-TT-TEO:PCB-TEO only obtains a low PCE of 2.8% with a dramatically reduced FF (**Figure 3** and **Table 3**). The poor performance should

be ascribed to the discontinuous film morphology caused by the poor solubility of PCB-TEO in organic solvents, as revealed by AFM observation (**Figure S7**).

Compatibilizer has been proved to be an effective approach to improve the formation of D/A nanoscale interpenetrating network. Since the PCB-TEO did not performed satisfactorily as an acceptor in the PSCs for its poor solubility, it could be used to serve as a compatibilizer in PBDTT-TT-TEO:PCBM blends to modify the nanostructure of the active layer. Considering that PCB-TEO contains the same segment to both PBDTT-TT-TEO and PCBM, the compatibility between the immiscible PBDTT-TT-TEO and PCBM will be enhanced via PCB-TEO preferentially located at donor and acceptor interface to span the heterojunction itself, consequently ensuring good miscibility in the system. The solar cell performance of PBDTT-TT-TEO:PCBM:PCB-TEO ternary system is provided in **Table 3** and **Figure 3**. As expected, with addition of an appropriate amount of PCB-TEO into PBDTT-TT-TEO:PCBM blend, the PCE of device dramatically increases. And the device with 5% loading of PCB-TEO achieves the highest PCE of 4.8%, with a J_{sc} of 12.18 mA/cm^2, a V_{oc} of 0.722V and a FF of 55.0%. Compared to the PBDTT-TT:PCBM device, the PCB-TEO compatibilizer promotes approximately 33% improvement in PCE, 24% improvement in FF and 10% improvement in J_{sc}. The enhanced FF is associated to the remarkably improved Rsh from 197.8 Ω cm^2 (without PCB-TEO compatibilizer) to 469.4 Ω cm^2 (with PCB-TEO compatibilizer). Further increasing the loading of PCB-TEO to 10% results in a sharp decrease in the overall parameters (PCE=4.0%, FF=50.2%, J_{sc} =11.03 mA/cm^2), except for the almost unchanged V_{oc} which is mainly determined by the difference between the HOMO of donor and LUMO of acceptor. In addition, PCB-TEO was also incorporated into the PBDTT-TT/PCBM blends without TEO for comparison, and the corresponding performance is showed in **Table S1 (Figure S8)**. Due to lack of TEO in PBDTT-TT donor, the PCB-TEO compatibilizer can not serve the same function on PBDTT-TT as on the PBDTT-TT-TEO. Therefore, the device only delivers a PCE of 3.2% for 3% loading of PCB-TEO and 2.7% for 5% loading of PCB-TEO.

From the device performance, it can be concluded that incorporation of TEO into the donor and acceptor can allow for the improved PCE by enhancing the J_{sc} and FF. **Figure 4** shows the UV-vis spectra of blend films of PBDTT-TT/PCBM, PBDTT-TT-TEO/PCBM and PBDTT-TT-TEO/PCBM with different amount of PCB-TEO. Compared with the PBDTT-TT/PCBM, PBDTT-TT-TEO/PCBM shows an obviously enhanced absorption intensity at 740~800nm, owning to the better arrangement favored by the TEO segment. When a small amount of PCBM is replaced by PCB-TEO from 3% to 10%, the absorption intensity further increase, and the blends with 5% and 10% ratio of PCB-TEO presents the strongest absorption at the solar flux region. This is because the PCB-TEO preferentially located at donor and acceptor interface favors the more ordered arrangements via the interaction between the same TEO side chains. The enhanced absorption peaks should be responsible for the enhanced J_{sc}.

No obvious distinction of X-ray diffraction patterns can be seen in **Figure 5** when blending the two polymers with PCBM. However, slightly increasing loading of the PCB-TEO additive from 3% to 10%, the crystalline diffraction peak at low angle becomes sharper and moves to the higher angle. The result indicates that the cooperative assembly between PBDTT-TT-TEO and PCB-TEO can enhance the crystallinity of polymer crystallites and form tighter packing of lamellar structure. The self-aggregation tendency induced by cooperative assembly of TEO side chains is essential for the hole and electron transport.

To gain a deeper insight into the morphologies of the active layers, the surfaces of the donor/acceptor blends by AFM have been studied (**Figure 6**). The PBDTTT-TT-TEO: PCBM film reveals a rough surface morphology with the root-mean-square (RMS) roughness of 1.12 nm at 1μm×1μm scan size. This obvious phase separation may produce poor contact between the active layer and the electrode, and yield unfavorable conditions for charge separation and transport. With addition of 3%

PCB-TEO into the film, a better surface morphology with the reduced RMS roughness of 0.93 nm is developed, while the best-optimized morphology can be acquired with the RMS roughness of 0.51 nm for the film with 5% PCB-TEO. As shown in **Figure 6**, the miscibility of PBDTTT-TT-TEO and PCBM is greatly enhanced, and PCBM is well dispersed in polymer matrix with addition of 5% PCB-TEO to the blend. The smooth and homogenous morphology can provide a nano-scale bi-continuous network of donor and acceptor materials for efficient charge dissociation and transportation, leading to a high PCE. The smoothest film with RMS roughness of 0.36 nm is obtained from the blend with 10% loading of PCB-TEO. However, too much PCB-TEO leads to large-size phase separation, as revealed by **Figure 6**. Therefore, a sharply decreased PCE was received. For PBDTT-TT:PCBM, without cooperation assembly of TEO side chains, only adding 3% PCB-TEO into the active layer produces a severely macrophase aggregation (**Figure S9**).

The morphologies of PBDTT-TT-TEO:PCBM and PBDTT-TT-TEO:PCBM:PCB-TEO (5% PCB-TEO) films are further detected by the planar transmission electron microscopy (TEM) (**Figure 7**). The bright and dark parts present the polymer-rich and PCBM-rich domains, respectively. The big PCBM clusters can be clearly distinguished from the dark area in the TEM image of PBDTT-TT-TEO:PCBM blends (**Figure 7**). In contrast, adding 5% PCB-TEO into the blends induces a homogeneous morphology of polymer and PCBM with equal domain size. Therefore, from the device performance, light absorption as well as the morphology, it is referred that incorporation of TEO side chain into the activelayer obviously improves the ordering degree of the blend film. More importantly, by precisely controlling the loadings of PCB-TEO, PCB-TEO can serve as an effective compatibilizer to well manipulate the miscibility between the donor and acceptor and the scale of the phase separation in PBDTT-TT-TEO:PCBM blend by cooperative assembly effect, consequently achieving a favorable BHJ morphology and improving the device performance. The schematic illustration of cooperative assembly structure of PBDTT-TT-TEO:PCBM: PCB-TEO has been depicted in **Scheme 3**.

Since PCB-TEO compatibilizer favors good miscibility of the PBDTT-TT-TEO and PCBM via interaction with TEO side chains and fullerene, the good morphological stability of the blends is also anticipated. **Figure 8** shows the variation of the performances of the devices with PBDTT-TT:PCBM (1:2 w/w), PBDTT-TT-TEO:PCBM (1:2 w/w) and PBDTT-TT-TEO:PCBM:PCB-TEO (1:1.90:0.10 w/w) annealed at 150 ^{o}C for different time in a glove box under N_2 atmosphere. The inert atmosphere is introduced to exclude the influence of humidity and oxygen and allow us to focus on the influence of morphological change on the device performance under elevated temperature. PBDTT-TT based devices show rapid degradation in the PCE, especially during the first 1 h (less than 70%), and only 25% of PCE remains after annealed for 8 h. However, both the PBDTT-TT-TEO based devices show better stability. The devices maintain 56% of the PCE for PBDTT-TT-TEO/PCBM devices and 75% of the PCE for the devices composed of PBDTT-TT-TEO and PCBM with 5% PCB-TEO after heated for 8 h. **Figure 9** shows the optical images of the morphology changes of PBDTT-TT:PCBM, PBDTT-TT-TEO:PCBM and PBDTT-TT-TEO:PCBM (5% PCB-TEO) films before and after annealed at 150 ^{o}C for 8 h. All of the films present homogeneous morphology without large PCBM crystals before thermal treatment. However, after annealed at 150 ^{o}C for 8 h, numerous needle-like PCBM crystals appear over the whole regions in PBDTT-TT based samples. This kind of large-scale macro-phase separation is the main reason for the deterioration of the device performance.[37, 38] In the thermal annealed PBDTT-TT-TEO/PCBM film, there are still some PCBM crystals. Nevertheless, for PBDTT-TT-TEO/PCBM/ PCB-TEO (5%) blend, due to the PCB-TEO compatibilizer located at the interface of donor and acceptor to strength the interaction of PBDTT-TT-TEO with PCBM, the formation of large PCBM crystals is found to be greatly suppressed, consequently leading to the enhanced thermal stability of the devices.[20, 39]

Conclusions

In summary, we have first presented a novel approach by introducing TEO functionalized copolymer donor PBDTT-TT-TEO and fullerene acceptor PCB-TEO together to manipulate the self-assembly nanoscale morphology and enhance stability of photoactive layer in polymer solar cells. Compared with the PBDTT-TT:PCBM blend, the PCE of PBDTT-TT-TEO:PCBM based device is improved from 3.6% to 4.1%, due to more ordered molecular packing induced by TEO side chains. However, directly blending PBDTT-TT-TEO with PCB-TEO as the activelayer affords poor performance due to the discontinuous morphology of blend film. Nevertheless, incorporation of a appropriate amount of the PCB-TEO as a compatibilizer into the PBDTT-TT-TEO:PCBM blend can effectively improve the device performance. The device with 5% loading of PCB-TEO achieves the highest PCE of 4.8%, with approximately 33% improvement in PCE, 24% improvement in FF and 10% improvement in J_{sc}. Because PCB-TEO, chemically similar to the segments in PBDTT-TT-TEO and PCBM, can locate at the interface of donor and acceptor to well manipulate the miscibility between the polymer and fullerene and achieve a favorable and stable BHJ morphology by cooperative assembly effect. In addition, good miscibility of the donor and acceptor helped by PCB-TEO greatly improves morphological stability of the blends and the thermally stability of the device. All of these features indicate that cooperative assembly of TEO functionalized copolymer and fullerene is a promising approach to develop well-defined and stable morphology of photoactive layer in polymer solar cells.

ACKNOWLEDGEMENTS

This work was supported by the National Natural Science Foundation of China (51273088 and 51263016).

REFERENCES

1. Krebs, F. C.; Fyenbo, J.; Jørgensen, M. *J. Mater. Chem.* **2010,** 20, (41), 8994-9001.
2. Helgesen, M.; Søndergaard, R.; Krebs, F. C. *J. Mater. Chem.* **2010,** 20, (1), 36-60.
3. Yip, H.-L.; Jen, A. K.-Y. *Energy Envir. Sci.* **2012,** 5, (3), 5994-6011.
4. Thompson, B. C.; Fréchet, J. M. J. *Angew. Chem. Inter. Ed.* **2008,** 47, (1), 58-77.
5. Arias, A. C.; MacKenzie, J. D.; McCulloch, I.; Rivnay, J.; Salleo, A. *Chem. Rev.* **2010,** 110, (1), 3-24.
6. Cheng, Y.-J.; Chen, C.-H.; Lin, Y.-S.; Chang, C.-Y.; Hsu, C.-S. *Chem. Mater.* **2011,** 23, (22), 5068-5075.
7. Murase, S.; Yang, Y. *Adv. Mater.* **2012,** 24, (18), 2459-2462.
8. Lin, Y.; Lim, J. A.; Wei, Q.; Mannsfeld, S. C.; Briseno, A. L.; Watkins, J. J. *Chem.Mater.* **2012,** 24, (3), 622-632.
9. Yao, K.; Chen, L.; Chen, X.; Chen, Y. *Chem. Mater.* **2013,** 25, (6), 897-904.
10. Du, C.; Li, C.; Li, W.; Chen, X.; Bo, Z.; Veit, C.; Ma, Z.; Wuerfel, U.; Zhu, H.; Hu, W. *Macromolecules* **2011,** 44, (19), 7617-7624.
11. Huo, L.; Zhang, S.; Guo, X.; Xu, F.; Li, Y.; Hou, J. *Angew. Chem. Inter. Ed.* **2011,** 123, (41), 9871-9876.
12. Chen, J.; Cao, Y. *Acc. Chem. Res.* **2009,** 42, (11), 1709-1718.
13. Chu, T.-Y.; Lu, J.; Beaupré, S.; Zhang, Y.; Pouliot, J.-R.; Wakim, S.; Zhou, J.; Leclerc, M.; Li, Z.; Ding, J. *J. Am. Chem. Soc.* **2011,** 133, (12), 4250-4253.
14. Cabanetos, C. m.; El Labban, A.; Bartelt, J. A.; Douglas, J. D.; Mateker, W. R.; Fréchet, J. M.; McGehee, M. D.; Beaujuge, P. M. *J. Am. Chem. Soc.* **2013,** 135, (12), 4656-4659.
15. Price, S. C.; Stuart, A. C.; Yang, L.; Zhou, H.; You, W. *J. Am. Chem. Soc.* **2011,** 133, (12), 4625-4631.
16. Graham, K. R.; Wieruszewski, P. M.; Stalder, R.; Hartel, M. J.; Mei, J.; So, F.; Reynolds, J. R. *Adv. Funct. Mater.* **2012,** 22, (22), 4801-4813.
17. Lee, J. K.; Ma, W. L.; Brabec, C. J.; Yuen, J.; Moon, J. S.; Kim, J. Y.; Lee, K.; Bazan, G. C.; Heeger, A. J. *J. Am. Chem. Soc.* **2008,** 130, (11), 3619-3623.
18. Liu, X.; Huettner, S.; Rong, Z.; Sommer, M.; Friend, R. H. *Adv. Mater.* **2012,** 24, (5), 669-674.
19. Jo, J.; Na, S.-I.; Kim, S.-S.; Lee, T.-W.; Chung, Y.; Kang, S.-J.; Vak, D.; Kim, D.-Y. *Adv. Funct. Mater.* **2009,** 19, (15), 2398-2406.
20. Jung, J. W.; Jo, J. W.; Jo, W. H. *Adv. Mater.* **2011,** 23, (15), 1782-7.
21. Chen, F.-C.; Chien, S.-C. *J. Mater. Chem.* **2009,** 19, (37), 6865-6869.
22. Jeng, J. Y.; Lin, M. W.; Hsu, Y. J.; Wen, T. C.; Guo, T. F. *Adv. Energy Mater.* **2011,** 1, (6), 1192-1198.
23. Shi, Y.; Li, F.; Chen, Y. *New J. Chem.* **2013,** 37, (1), 236-244.
24. Søndergaard, R.; Helgesen, M.; Jørgensen, M.; Krebs, F. C. *Adv. Energy Mater.* **2011,** 1, (1), 68-71.
25. Lu, K.; Fang, J.; Zhu, X.; Yan, H.; Li, D.; Yang, Y.; Wei, Z. *New J. Chem.* **2013**.
26. Kanimozhi, C.; Yaacobi-Gross, N.; Chou, K. W.; Amassian, A.; Anthopoulos, T. D.; Patil, S. *J. Am. Chem. Soc.* **2012,** 134, (40), 16532-16535.
27. McCullough, R. D. *Adv. Mater.* **1998,** 10, (2), 93-116.
28. Paci, B.; Generosi, A.; Albertini, V. R.; Generosi, R.; Perfetti, P.; Bettignies, R. d.; Sentein, C. *J.*

Phys. Chem. C **2008,** 112, (26), 9931-9936.

29. Manceau, M.; Helgesen, M.; Krebs, F. C. *Polym. Degrad. Stab.* **2010,** 95, (12), 2666-2669.

30. Kim, B. J.; Miyamoto, Y.; Ma, B.; Fréchet, J. M. J. *Adv. Funct. Mater.* **2009,** 19, (14), 2273-2281.

31. Huang, F.; Cheng, Y.-J.; Zhang, Y.; Liu, M. S.; Jen, A. K. Y. *J. Mater. Chem.* **2008,** 18, (38), 4495-4509.

32. Qian, D.; Xu, Q.; Hou, X.; Wang, F.; Hou, J.; Tan, Z. a. *J. Polym. Sci. Part A: Polym. Chem.* **2013,** 51, (15), 3123-3131.

33. Liu, H.-W.; Chang, D.-Y.; Chiu, W.-Y.; Rwei, S.-P.; Wang, L. *J. Mater. Chem.* **2012,** 22, (31), 15586-15591.

34. Roncali, J.; Marque, P.; Garreau, R.; Garnier, F.; Lemaire, M. *Macromolecules* **1990,** 23, (5), 1347-1352.

35. Chen, L.; Li, X.; Chen, Y. *Polym. Chem.* **2013,** 4, (23), 5637-5644.

36. Han, D.; Tong, X.; Zhao, Y.; Zhao, Y. *Angew. Chem. Inter. Ed.* **2010,** 122, (48), 9348-9351.

37. Swinnen, A.; Haeldermans, I.; vande Ven, M.; D'Haen, J.; Vanhoyland, G.; Aresu, S.; D'Olieslaeger, M.; Manca, J. *Adv.Funct. Mater.* **2006,** 16, (6), 760-765.

38. Woo, C. H.; Thompson, B. C.; Kim, B. J.; Toney, M. F.; Fréchet, J. M. J. *J. Am. Chem. Soc.* **2008,** 130, (48), 16324-16329.

39. Tai, Q.; Li, J.; Liu, Z.; Sun, Z.; Zhao, X.; Yan, F. *J. Mate. Chem.* **2011,** 21, (19), 6848-6853.

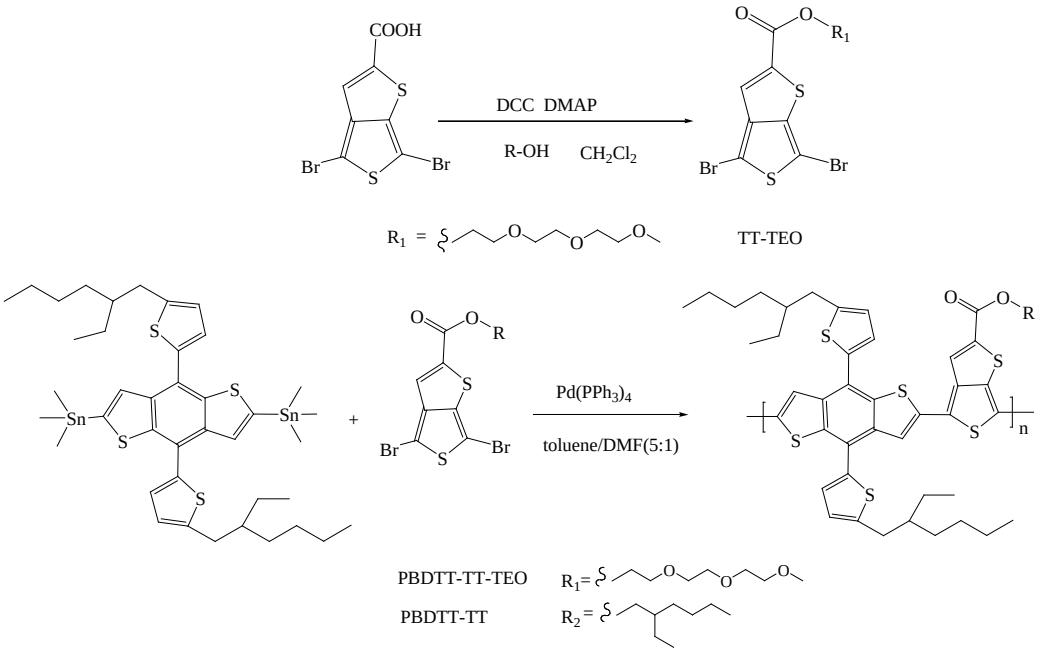

Scheme 1. Synthetic routes for polymers PBDTT-TT-TEO and PBDTT-TT.

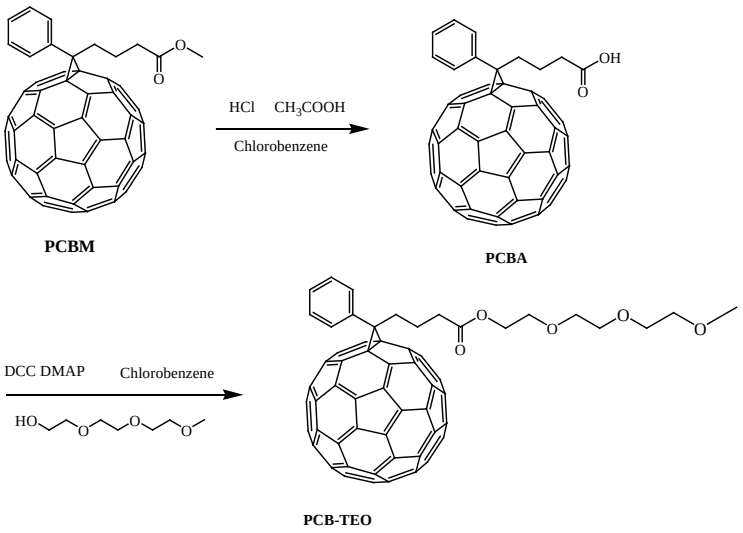

Scheme 2. Synthetic routes for PCB-TEO.

Table 1. Physical properties and photoelectric data for PBDTT-TT and PBDTT-TT-TEO

Polymer	T_d (^oC)	M_n (kg/mol)	PDI	λ_{max} (nm)	E_g^{opt}/E_g^{CV} (eV)	E_{HOMO} (eV)	E_{LUMO} (eV)
PBDTT-TT	364	20.5	3.1	696	1.61/1.87	-5.09	-3.22
PBDTT-TT-TEO	366	21.3	2.8	701	1.58/1.85	-5.07	-3.23

E_{HOMO} = -(Eox + 4.8) eV and E_{LUMO} = -(Ered + 4.8) eV. The electrochemical band gap (E_g^{CV}) was calculated on the formula, $E_g^{CV} = E_{LUMO} - E_{HOMO}$.

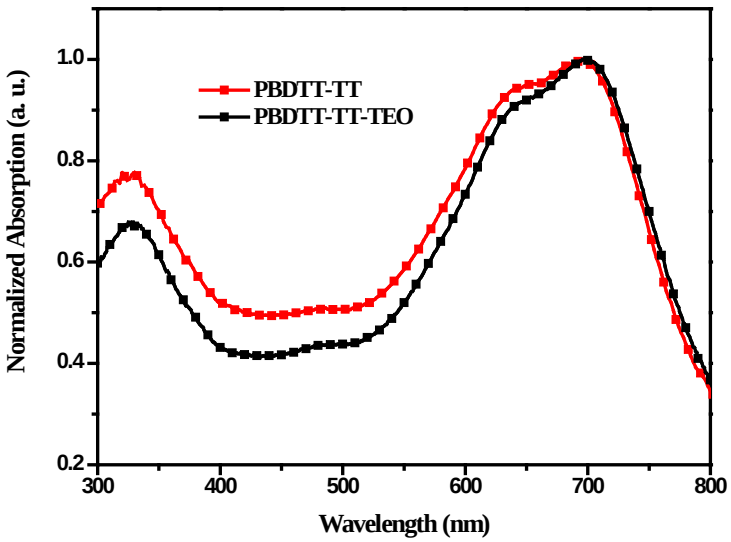

Figure 1. UV-vis spectra of PBDTT-TT and PBDTT-TT-TEO films.

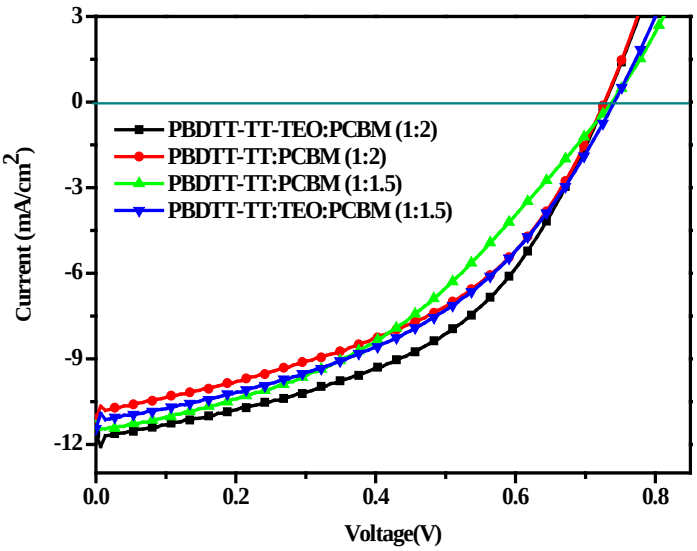

Figure 2. J-V curves of PBDTT-TT-TEO:PCBM (1:2 w/w), PBDTT-TT:PCBM (1:2 w/w), PBDTT-TT:PCBM (1:1.5 w/w) and PBDTT-TT-TEO:PCBM (1:1.5w/w) solar devices.

Table 2. Solar Cell Performance Parameters of PBDTT-TT:PCBM (1:2 w/w), PBDTT-TT-TEO:PCBM (1:2 w/w), PBDTT-TT:PCBM (1:1.5 w/w) and PBDTT-TT-TEO:PCBM (1:1.5 w/w) Blends

PV Devices	blend ratio polymer:PCBM	V_{oc} (V)	J_{sc} (mA/cm^2)	FF (%)	R_s (Ω cm^2)	R_{sh} (Ω cm^2)	PCE (%)[a]
PBDTT-TT	1:2	0.726	11.09	44.5	15.8	187.6	3.6
PBDTT-TT-TEO	1:2	0.727	11.63	48.1	15.2	197.8	4.1
PBDTT-TT	1:1.5	0.735	11.39	40.8	99.6	254.4	3.4
PBDTT-TT-TEO	1:1.5	0.741	11.44	43.1	12.9	216.8	3.7

[a)] All values represent averages.

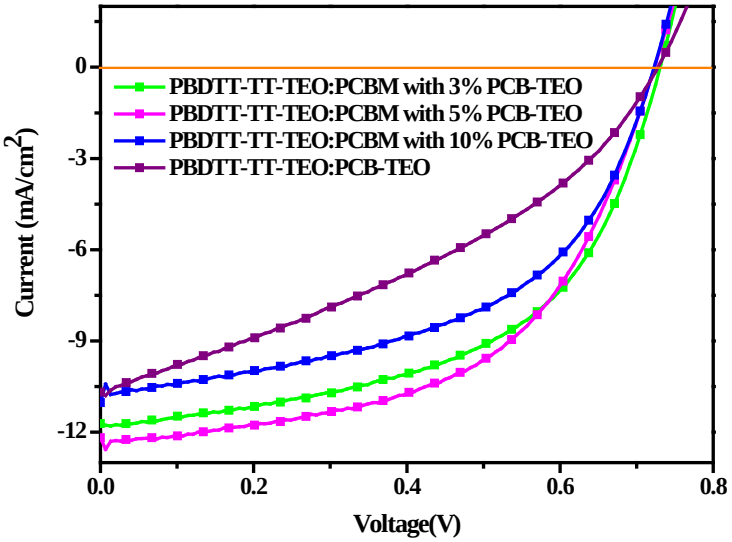

Figure 3. J-V curves of PBDTT-TT-TEO/PCBM solar devices in which various amount of PCBM is replaced with PCB-TEO.

Table 3. Solar Cell Performance Parameters of PBDTT-TT-TEO: PCBM with different ratio of PCB-TEO

PV Devices [a]	V_{oc} (V)	J_{sc} (mA/cm^2)	FF (%)	R_s (Ω cm^2)	R_{sh} (Ω cm^2)	PCE (%) [b]
3% PCB-TEO	0. 729	11.72	54.2	128.6	390.6	4.5
5% PCB-TEO	0.722	12.18	55.0	17.8	469.4	4.8
10% PCB-TEO	0.722	11.03	50.2	11.1	265.4	4.0
100% PCB-TEO	0.725	10.69	36.1	8.6	104.9	2.8

[a)]Weight ratio to the total amount of PCB-TEO and PCBM (blended with BDTT-TT-TEO); [b)]All values represent averages.

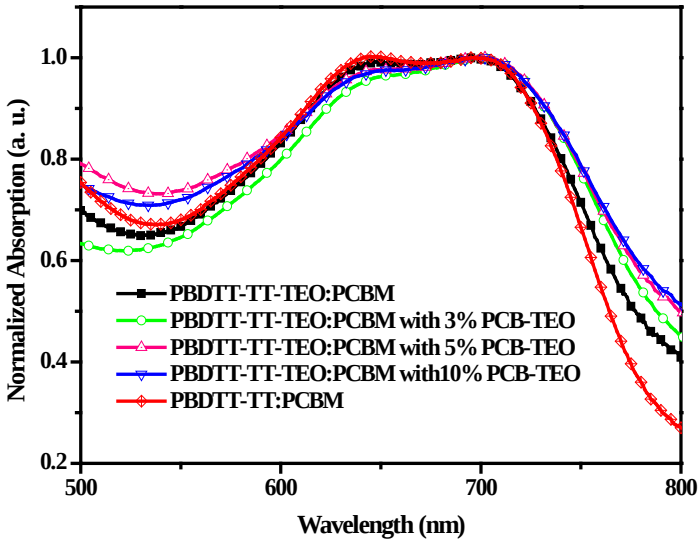

Figure 4. UV-vis spectra of blend films of PBDTT-TT:PCBM and PBDTT-TT-TEO:PCBM with different amounts of PCB-TEO.

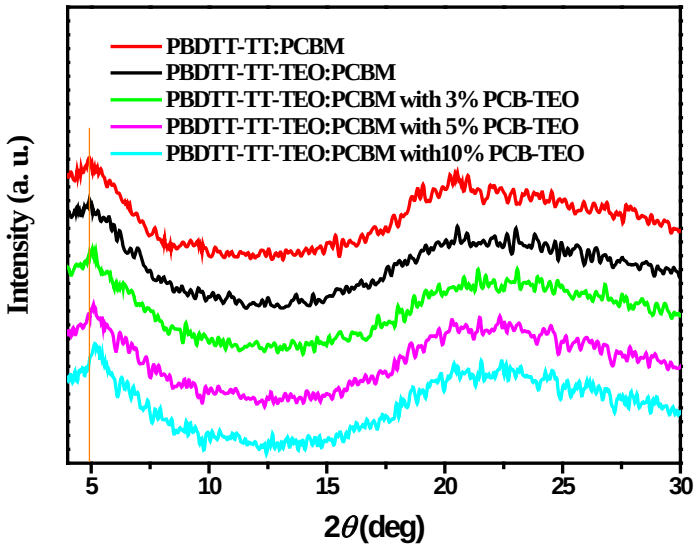

Figure 5. X-ray diffraction patterns of PBDTT-TT:PCBM and PBDTT-TT-TEO:PCBM with different amounts of PCB-TEO.

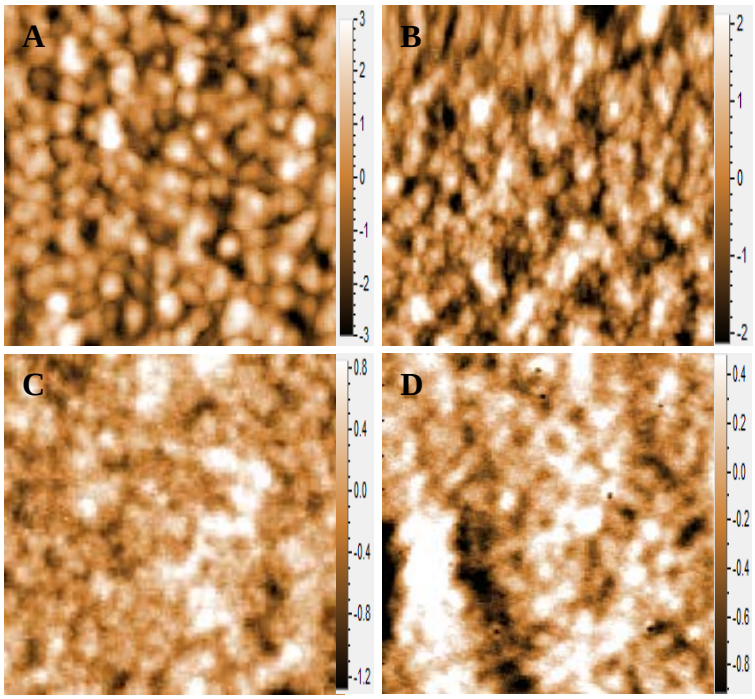

Figure 6. AFM topography mages (1μm × 1 μm) of PBDTT-TT-TEO:PCBM films in which (A) without, (B) 3%, (C) 5%, and (D) 10% of PCBM is replaced with PCB-TEO.

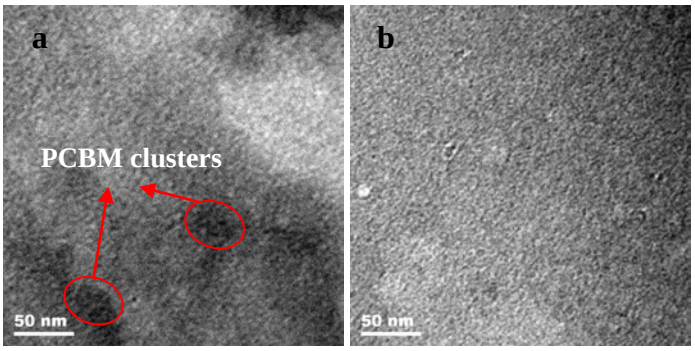

Figure 7. TEM images of (a) PBDTT-TT-TEO:PCBM and (b) PBDTT-TT-TEO:PCBM with 5% PCB-TEO.

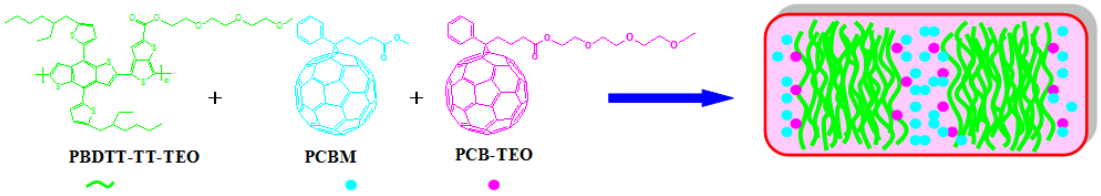

Scheme 3. Schematic of PCE-TEO as compatibilizer in PBDTT-TT-TEO:PCBM blend to mediate the interfacial contact and BHJ morphology.

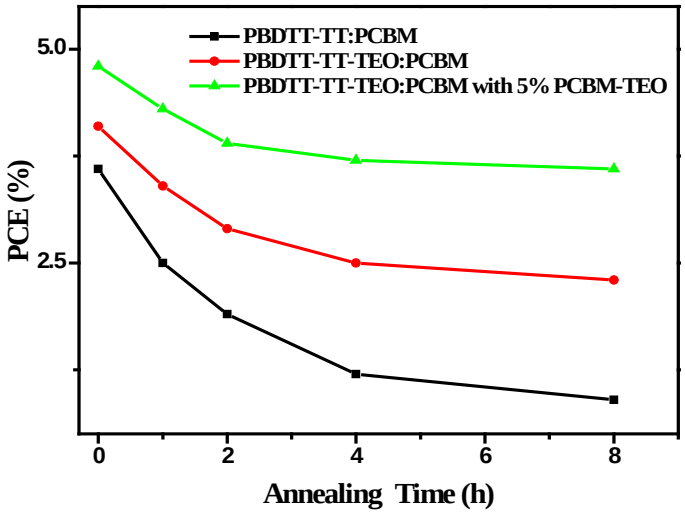

Figure 8. Time dependence of efficiencies of the PSCs based on PBDTT-TT:PCBM, PBDTT-TT-TEO:PCBM, and PBDTT-TT-TEO:PCBM with 5% PCB-TEO after annealing at 150 ^{o}C.

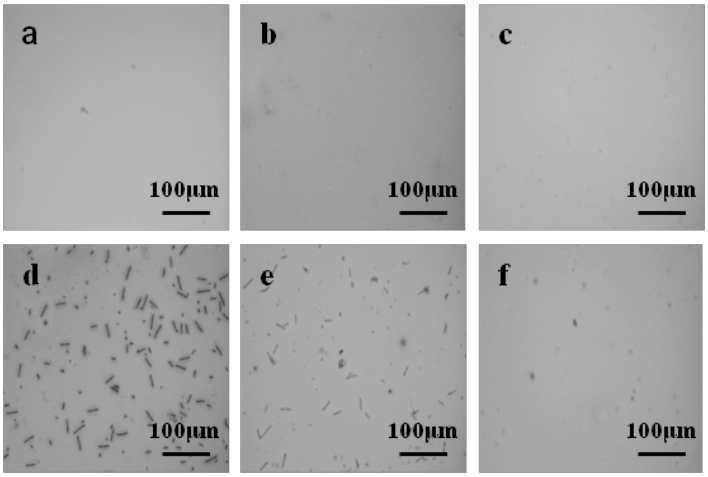

Figure 9. Optical micrographs of thin films of PBDTT-TT: PCBM (a, d), PBDTT-TT-TEO:PCBM (b, e), and PBDTT-TT-TEO:PCBM with 5% PCB-TEO (c, f) before (a, b, c) and after annealing (d, e, f) at 150 ^{o}C for 8 h. The dark areas correspond to PCBM rich domains.

Table of Content

Enhanced Performance for Organic Bulk Heterojunction Solar Cells by Cooperative Assembly of Ter(ethylene Oxide) Pendant

Lie Chen, Shaojie Tian, Yiwang Chen

Two ter(ethylene oxide) funtionalized donor and acceptor are explored to manipulate self-assembly morphology of photoactive layer in polymer solar cells.